

Geochemical characteristics and significance of major elements, trace elements and REE of NM copper polymetal deposit in Laos

JIA Runxing (贾润幸)^{1,2,3}, FANG Weixuan (方维萱)^{1,2}, HU Ruizhong (胡瑞忠)¹

(1. Key Laboratory of Ore Deposit Geochemistry, Institute of Geochemistry, Chinese Academy of Sciences, Guiyang 550002, China; 2. Beijing Exploration Technology Center for Mineral Resources, China Non-Ferrous Metals Resource Geological Survey, Beijing 100012, China; 3. Beijing Donia Resources Co., Ltd., Beijing 100012, China)

Received 6 July 2009; revised 27 July 2009

Abstract: The NM copper polymetal deposit is located in the middle north part of the Truong Son metallogenic belt in Laos, which is the skarn-typed deposit and located in the contact between Indosinian granite and Lower Carboniferous limestone. All the ore-bodies in NM deposit can be divided into four types according to their occurrences: I copper ore-body as the massive restite developed in inner contact near the granite in north part; II-1 zinc-copper ore body and II-2 copper-iron ore body developed within contact between the granite and carbonate rocks, III copper-zinc ore body developed in the cranny among the southern carbonate stratum, indicating that all the ore-bodies were related to Indosinian granite emplacing into the Carboniferous limestone and causing the metallogenic system from closed state getting into half open state. The geochemical characteristics and mineral assemblages of them showed that all the orebodies in NM deposit derived from a similar origin and their ore-forming fluids with the evolution trend from reductive state in early stage to oxidative state in later stage were mainly related to the coupling interaction between post-magmatic hydrothermal fluid and basin fluid.

Keywords: rare earth elements; copper polymetal deposit; skarn; Laos

Laos is located in the southern part of Sanjiang metallogenic belt extending from south China to southeast Asia^[1,2]. In recent decades, some world-class deposits i.e. Phu Kham Cu-Au deposit and Sepon Cu-Au deposit have been discovered and estimated in this area, which caused Laos one of the most prospective areas for metal exploration in the world. NM copper polymetal deposit is located approximately 40 km east of the Phu Kham Cu-Au deposit in Xaisomboun district, Vientiane Province, Lao PDR. The metallogenic background and geological conditions for NM deposit are very well and similar to Phu Kham Cu-Au deposit. Previous studies^[3,4] were mainly focused on the metallogenic belt or the geological setting in whole Laos, and the fundamental geology of this area in Xaisomboun district was not detailed. In this paper, based on the field works and the analysis results of major elements, trace elements and rare earth elements for orebodies in different occurrences of the NM copper polymetallic deposits, the spatial distribution laws for different orebodies and their relationship in genesis were discussed so as to provide some usefully theoretical basis and help us do appropriate exploration for new targets in this area.

1 Geological setting

The geotectonic position of NM copper polymetal deposit

is located on the junction between North-East trending Louangphabang tectonic belt and North-West trending Truong Son tectonic belt in Laos. Indosinian biotite granite emplaced into the Carboniferous carbonate rock and Jurassic siltstones in multi-stage and formed nearly East-West trending Xaisomboun fault and some subfault along the southern part of NM area. All the orebodies developed within or near the contact between granite and carbonate rock can be divided into four types according to their occurrences and the mineral aggregate: I copper ore-body as the massive restite developed in inner contact near the granite on north part; II-1 zinc-copper ore body and II-2 copper-iron ore body as lenticular or multilayered occurrences developed within contact between the granite and carbonate rocks; III copper-zinc ore body comprised by some small lodes developed in the cranny among the southern carbonate stratum (Fig. 1).

I copper-zinc orebody mainly consists of chalcopyrite, marcasite, pyrrhotite and minor pyrite, sphalerite, tetrahedrite, bismuthinite and matrix minerals of quartz, diopside, chlorite. II-1 zinc-copper orebody mainly comprises chalcopyrite, sphalerite, galena, pyrite and their oxides, i.e. limonite and covellite disseminated among the intervals of skarn minerals including hedenbergite, diopside, tremolite, garnet, epidote, biotite, quartz, fluorite and calcite. II-2 copper-iron orebody comprises pyrrhotite, magnetite, chalcopyrite, covellite, pyrite, marcasite, hematite, limonite disseminated

Foundation item: Project supported by China Postdoctoral Science Foundation, Institute of Geochemistry under Chinese Academy of Sciences and "Research of quick-locating-technical methods for Xaisomboun metallogenic target in Laos", a innovative fund of China non-ferrous Metals Resource Geological Survey

Corresponding author: Fang Weixuan (E-mail: fangwuxuan@tom.com; Tel.: +86-10-84928604)

DOI: 10.1016/S1002-0721(09)60102-2

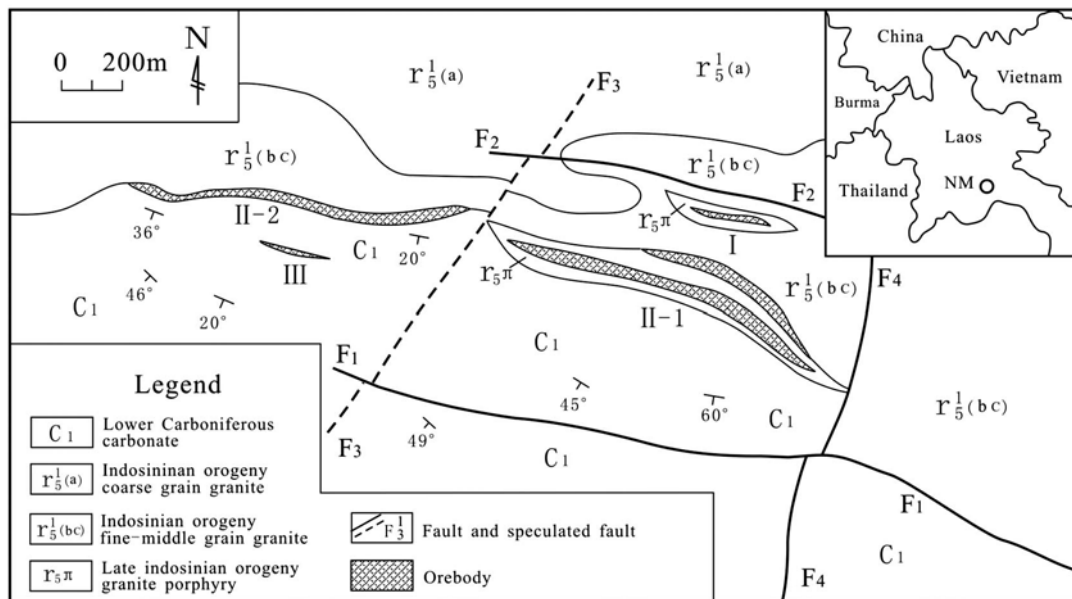


Fig. 1 Geological map of NM Copper polymetal deposit in Vientiane Province, Laos

among the intervals of skarn minerals including garnet, hedenbergite, diopside, tremolite and a small quantity of other minerals (calcite, sericite and biotite). III copper-zinc orebody mainly consists of chalcopyrite, sphalerite, bornite, and minor galena disseminated among intervals of skarn minerals including idocrase, wollastonite, garnet and diopside.

2 Sampling and analysis

In order to study the geochemical characteristics of NM copper polymetallic deposit, different typical ore samples were collected and each sample weighed about 500 g during the site sampling. After the samples were cut and polished into thin sections, the fresh part of samples without oxide and alteration were crushed to less than 0.25 mm in a jaw crusher, quartered, pulverized in disc crusher to less than 0.095 mm. Finally, prepared samples weighed more than 100 g. The analyses were carried out at Analytical Laboratory Beijing Research Institute of Uranium Geology, major element were analyzed by X-ray fluorescence spectroscopy method, trace element and REE were analyzed by ICP-MS method^[5] (data listed in Table 1).

3 Geochemical characteristics of ores

3.1 Major element

As shown in Fig. 2, I ore samples have lower concentrations of SiO_2 and CaO and higher concentrations of FeO and Fe_2O_3 , which are related to the existence of pyrrhotite, pyrite and other sulfides in the ore rock; II-1 ore sample have higher concentrations of SiO_2 and CaO due to the higher contents of quartz and hedenbergite; the higher concentrations of FeO and Fe_2O_3 in II-2 ore sample are related to the higher content of magnetite; the higher concentrations of CaO , SiO_2 and Al_2O_3 in III ore sample are mainly related to

the high contents of idocrase, calcite and other skarn minerals.

3.2 Trace elements

As shown in Fig. 3, the incompatible elements of all ore samples normalized by primitive mantle^[6] display distinct fractionation of large ion lithophile elements (LILE: Cs, Rb, K, Th, U, Sr, Ba, and La) and high field strength elements (HFSE: Nb, Ta, Hf, and Ti). Sample from I orebody, II-1 orebody and II-2 orebody have the similar variation with enrichment of Cs, Rb, Th, U, Hf and depletion of Ba and Nb; Sample from III orebody occurred in the cranny among the carbonate stratum mainly enriched Th, U, Ta, La and depleted Rb, Ba, K, Nb, Sr, and Ti. The geochemical characteristics of incompatible element for different orebodies show that LILE of Cs, Rb were enriched nearby contact between granite, and carbonate rock vs LILE of La, Ce, Nd were enriched apart from the contact and near the country rock of carbonate, which may be related to the different ore-forming environment.

3.3 Associated metal elements

As shown in Fig. 4, all the orebodies have high concentrations of other associated metal elements in NM deposit, which is very similar to other skarn-type deposit in China^[7].

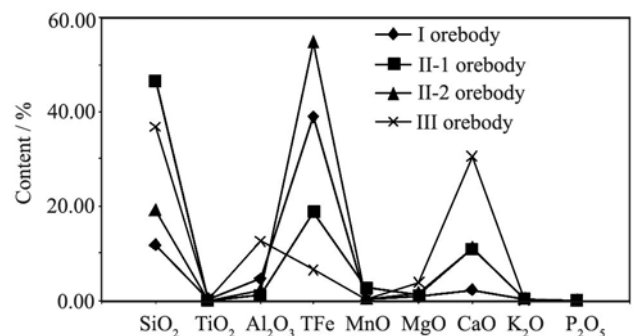


Fig. 2 Variety graph of average content of major element for different ore bodies in NM deposit

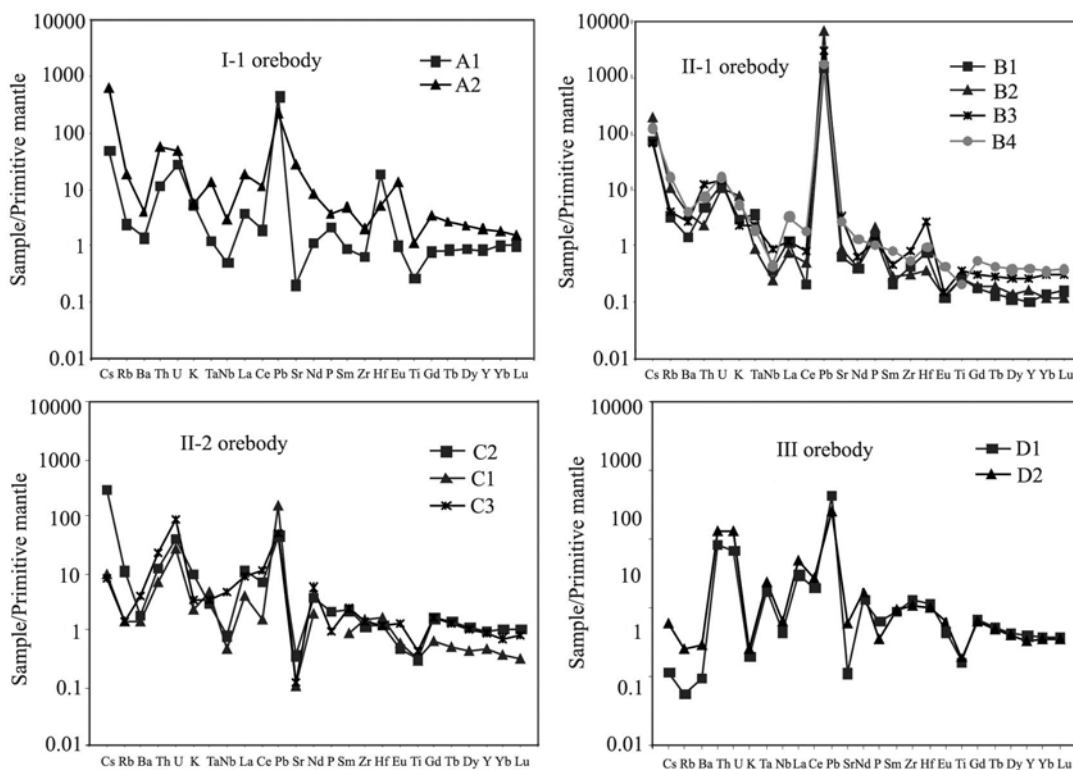


Fig. 3 Spider diagram of incompatible elements normalized by primitive mantle for different ore bodies

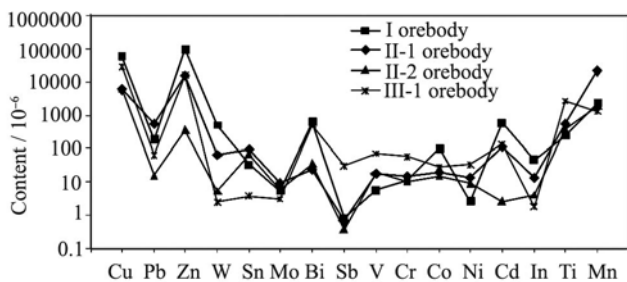


Fig. 4 Variety graph of average contents of associated metal elements for different ore bodies

W and Bi concentrations in sample A1 from I copper-zinc orebody are up to 1027×10^{-6} and 1239×10^{-6} , respectively; Cd concentration from II-1 zinc-copper orebody varies from 39.4×10^{-6} to 1140×10^{-6} with the average concentration of 379×10^{-6} . Bi and Cd concentrations in sample D1 from III copper-zinc orebody are up to 1002×10^{-6} and 267×10^{-6} , respectively. These useful elements associated with the main elements in different orebody could be utilized comprehensively in the future.

3.4 Rare earth elements

REE abundances for different ores are presented in Table 1 and their chondrite-normalized^[8] patterns are shown in Fig. 5. REE concentrations in I orebody range from 11.04×10^{-6} to 58.53×10^{-6} (average 34.79×10^{-6}) and are characterized by obvious fractionation of LREE and HREE with ratios of $\Sigma Ce/\Sigma Y$ and $(La/Yb)_N$ from 3.5×10^{-6} to 7.87×10^{-6} (average 5.69) and 3.54×10^{-6} to 9.51×10^{-6} (average 6.52×10^{-6}), respectively, unobviously negative Ce anomaly with δ_{Ce} varying from 0.964 to 1.03 (average 0.831) and obviously posi-

tive Eu anomaly with δ_{Eu} varying from 1.17 to 3.25 (average 2.21). The degree of LREE fractionation with ratio of $(La/Sm)_N$ from 3.69×10^{-6} to 4.09×10^{-6} (average 3.89×10^{-6}) is slightly higher than that of HREE with ratio of $(Gd/Yb)_N$ from 0.80×10^{-6} to 1.90×10^{-6} (average 1.35×10^{-6}).

II-1 orebody has lower concentrations of REE ranging from 2.38×10^{-6} to 9.54×10^{-6} (average 4.77×10^{-6}), and it is characterized by obvious fractionation of LREE and HREE with ratios of $\Sigma Ce/\Sigma Y$ from 4.68 to 7.26 (average 5.78), ratio of $(La/Yb)_N$ from 3.74×10^{-6} to 8.94×10^{-6} (average 6.63×10^{-6}), slightly negative Ce anomaly with δ_{Ce} varying from 0.259 to 0.827 (average 0.646), and obviously negative Eu anomaly with δ_{Eu} varying from 0.396 to 0.652 (average 0.551). Compared with HREE, the degree of LREE fractionation with ratio of $(La/Sm)_N$ from 2.55×10^{-6} to 5.28×10^{-6} (average 3.65×10^{-6}) is clearly higher than that of HREE with ratio of $(Gd/Yb)_N$ from 0.95×10^{-6} to 1.61×10^{-6} (average 1.32×10^{-6}).

REE concentrations in II-2 orebody range from 10.56×10^{-6} to 39.27×10^{-6} (average 26.79×10^{-6}), characterized by obvious fractionation of LREE and HREE with ratios of $\Sigma Ce/\Sigma Y$ from 7.54 to 12.55 (average 9.46), ratio of $(La/Yb)_N$ from 9.74×10^{-6} to 11.29×10^{-6} (average 10.77×10^{-6}), obviously negative Eu anomaly with δ_{Eu} varying from 0.240 to 0.786 (average 0.558), and Ce anomaly with δ_{Ce} varying from 0.443 to 1.162 (average 0.824). The degree of LREE fractionation with ratio of $(La/Sm)_N$ from 3.45×10^{-6} to 4.65×10^{-6} (average 4.21×10^{-6}) is slightly higher than that of HREE with ratio of $(Gd/Yb)_N$ from 1.48×10^{-6} to 2.37×10^{-6} (average 1.88×10^{-6}).

Compared with the above orebodies, III orebody has the highest concentrations of REE ranging from 99.12×10^{-6} to

Table 1 Major element content (%) and trace element ($\times 10^{-6}$) analysis result for different ore bodies in NM deposit*

Orebody	I Cu-Zn orebody		II-1 Zn-Cu orebody				II-2 Cu-Fe orebody			III Cu-Zn orebody	
Sample	A1	A2	B1	B2	B3	B4	C1	C2	C3	D1	D2
SiO ₂	15.37	8.11	54.61	45.16	58.56	28.5	6.79	15.37	34.85	32.45	41.09
TiO ₂	0.058	0.238	0.06	0.056	0.078	0.045	0.067	0.07	0.09	0.37	0.42
Al ₂ O ₃	3.95	5.28	0.4	1.45	1.025	1.198	1.6	2.07	2.49	10.78	14.18
Fe ₂ O ₃	20.41	36.64	6.01	5.54	4.64	9.63	66.12	19.05	30.65	4.31	3.04
FeO	11.05	9.88	2.22	20.78	7.56	19.2	16.87	26.85	5.05	4.65	1.34
MnO	0.18	0.23	0.45	3.40	2.08	4.57	0.15	0.36	0.15	0.13	0.17
MgO	0.67	0.94	0.15	1.55	1.18	1.44	1.15	1.62	2.13	2.72	4.80
CaO	0.66	3.70	1.72	18.55	8.23	14.76	2.58	7.53	23.47	29.96	31.27
Na ₂ O	—	—	<0.10	<0.10	—	—	<0.10	—	0.03	<0.10	0.11
K ₂ O	0.166	0.161	0.09	0.23	0.071	0.169	0.068	0.30	0.1	0.06	0.08
P ₂ O ₅	0.047	0.079	0.03	0.047	0.026	0.024	—	0.05	0.021	0.14	0.076
Ignition loss	11.9	1.86	6.84	—	3.06	0.44	—	1.58	0.2	—	2.96
S	7.85	18.40	—	—	1.54	0.31	—	4.68	—	—	—
V	9.72	41.6	1.63	10.2	9.02	12.1	18.1	13.9	25.4	62.2	76.9
Cr	8.03	42.4	13.3	2.65	9.16	4.9	6.33	19.4	5.79	38.1	76.8
Co	98.4	23.8	108	35.4	15.1	3.73	18.9	13.6	12.7	36.2	18.5
Ni	3.07	28.1	2	8.5	10.1	9.47	3.5	4.63	17.5	21	43.2
Cu	104603	1739	15261	934	21479	276	1585	9721	7200	52275	3788
Zn	3266	5718	189826	5280	13930	34715	509	273	299	32289	451
Ga	9.29	17.4	1.9	14.5	5.34	13.4	7.67	28.1	11.6	11.4	14.2
As	4.76	57.7	0.812	4.53	5.1	5.39	25.6	4.56	36.1	176	161
Se	3.05	1.95	4.06	0.145	0.406	0.748	0.751	0.576	0.208	3.9	0.247
Rb	1.55	11.5	2.15	6.63	2.59	10.8	0.868	7.07	0.935	0.357	1.68
Sr	4.21	591	14.2	18.3	71.5	61.8	2.33	7.54	2.55	23.9	124
Y	3.87	9.25	0.463	0.75	1.21	1.86	2.11	4.4	4.08	18.1	15.5
Zr	7.17	22.4	4.9	3.53	9.36	6.21	17.5	13.2	16.5	147	120
Nb	0.368	2.18	0.27	0.176	0.641	0.313	0.334	0.587	3.25	3.24	4.62
Mo	9.8	33.9	0.963	0.776	1.55	1.5	4.28	12.4	1.01	0.509	5.63
Cd	35.5	62.8	1140	39.4	96.8	241	3.56	1.67	2.49	267	1.27
In	86.5	48.6	8.98	2.43	0.998	0.693	2.61	3.87	5.51	3.54	0.189
Sn	59.7	360	3.18	17.9	2.31	3.3	87.1	25.1	84.2	2.51	4.68
Sb	0.399	0.345	1.24	0.799	0.932	0.578	0.469	0.608	0.055	11.7	47.8
Cs	1.54	19.1	2.44	6.3	2.27	4.04	0.297	9.69	0.257	0.038	0.195
Ba	9.87	28.7	10.3	26.7	19.4	29.3	10.1	12.8	28.8	6.73	20.8
Hf	5.78	1.64	0.244	0.111	0.903	0.306	0.528	0.385	0.374	3.55	3.15
Ta	0.051	0.553	0.15	0.038	0.096	0.08	0.182	0.123	0.137	0.748	1.01
W	1027	120	18.9	2.52	116	27.4	7.09	7.02	2.39	2.98	1.88
Re	0.064	0.008	0.002	0.001	0.006	0.003	0.001	0.002	0.001	0.001	0.001
Tl	0.021	0.127	0.014	0.051	0.115	0.042	0.02	0.059	0.015	0.01	0.028
Pb	79.9	41.6	298	1295	582	328	28.7	8.21	9.18	80.8	47.6
Bi	1239	32.4	11.2	5	10.4	46.6	45.4	4.04	58.4	1002	43.3
Th	0.997	4.75	0.424	0.2	1.09	0.653	0.588	1.02	1.97	7.13	10.8
U	0.589	0.968	0.264	0.217	0.311	0.354	0.558	0.842	1.93	1.5	2.72
Ti	361	1483	134	109	381	217	291	359	485	2075	3268
Ge	1.73	2.59	0.274	1.65	0.48	1.36	5.78	5.01	2	1.27	1.33
La	2.58	12.6	0.822	0.519	0.844	2.36	2.88	7.47	5.87	21.6	33.8
Ce	3.51	21.5	0.378	0.891	1.48	3.3	2.67	12.2	19	36.3	50.4
Pr	0.438	2.82	0.15	0.149	0.22	0.504	0.732	1.53	2.64	4.89	6.72
Nd	1.5	10.6	0.543	0.581	0.898	1.79	2.54	4.97	7.57	18.7	23.5
Sm	0.397	2.15	0.098	0.126	0.208	0.355	0.4	1.01	1.07	3.99	4.31
Eu	0.168	2.26	0.02	0.022	0.025	0.073	0.1	0.077	0.222	0.778	1.07
Gd	0.485	2.1	0.106	0.116	0.179	0.33	0.378	0.951	1.03	3.96	3.83
Tb	0.093	0.287	0.015	0.02	0.031	0.047	0.053	0.154	0.138	0.567	0.54
Dy	0.655	1.72	0.087	0.1	0.195	0.288	0.325	0.843	0.728	3.27	3.05
Ho	0.148	0.345	0.017	0.023	0.049	0.07	0.063	0.175	0.142	0.676	0.607
Er	0.435	1	0.054	0.064	0.135	0.187	0.195	0.495	0.391	1.96	1.78
Tm	0.07	0.14	0.008	0.009	0.021	0.027	0.026	0.078	0.059	0.276	0.25
Yb	0.492	0.893	0.071	0.058	0.152	0.178	0.172	0.517	0.351	1.87	1.72
Lu	0.072	0.114	0.012	0.009	0.024	0.028	0.024	0.08	0.06	0.28	0.26
ΣREE	11.04	58.53	2.38	2.69	4.46	9.54	10.56	30.55	39.27	99.12	131.84
ΣLREE	8.59	51.93	2.01	2.29	3.68	8.38	9.32	27.26	36.37	86.26	119.80
ΣHREE	2.45	6.60	0.37	0.40	0.79	1.16	1.24	3.29	2.90	12.86	12.04
ΣCe/ΣY	3.51	7.87	5.44	5.73	4.68	7.26	7.54	8.28	12.55	6.71	9.95
(La/Yb) _N	3.54	9.51	7.81	6.03	3.74	8.94	11.29	9.74	11.27	7.79	13.25
(La/Sm) _N	4.09	3.69	5.28	2.59	2.55	4.18	4.53	4.65	3.45	3.41	4.93
(Gd/Yb) _N	0.795	1.90	1.21	1.61	0.950	1.50	1.77	1.48	2.37	1.71	1.80
δ _{Ce}	0.795	0.868	0.259	0.771	0.827	0.728	0.443	0.869	1.16	0.850	0.805
δ _{Eu}	1.17	3.25	0.600	0.556	0.396	0.652	0.786	0.240	0.647	0.598	0.805

* indicates that data are below the detection limit

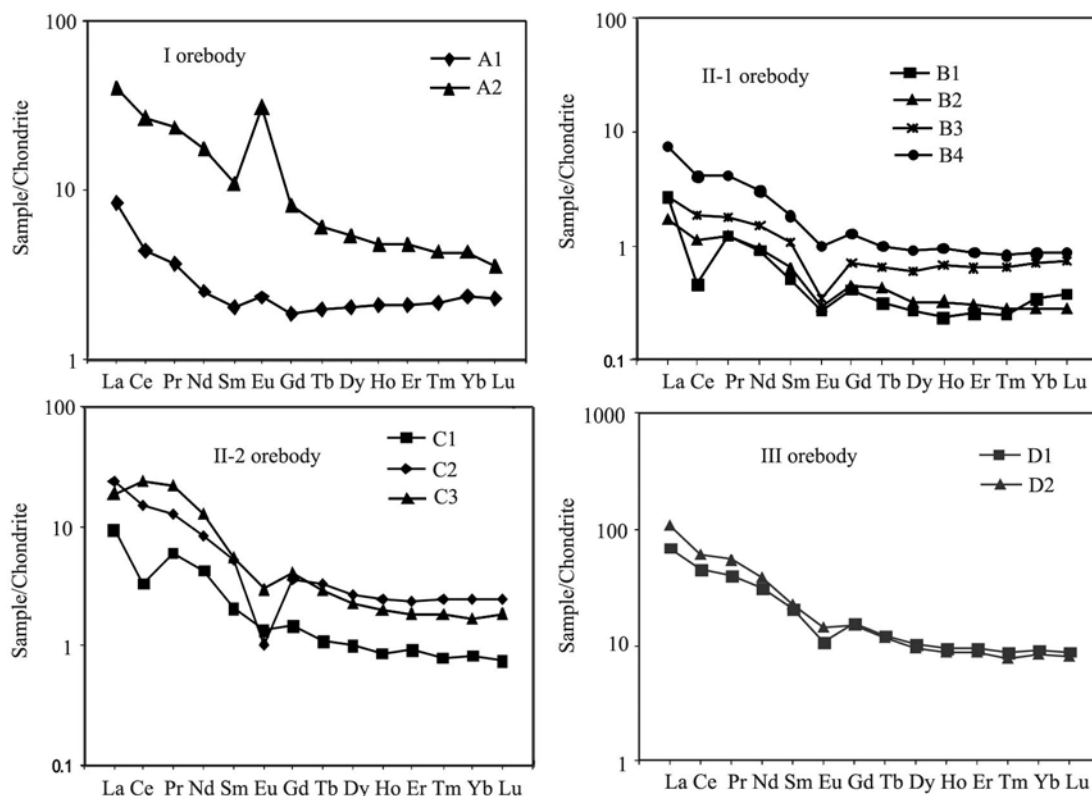


Fig. 5 Chondrite-normalized REE distribution patterns for different ore bodies

131.84×10^{-6} (average 115.48×10^{-6}), and it is characterized by obvious fractionation of LREE and HREE with ratios of $\Sigma Ce/\Sigma Y$ from 6.71 to 9.95 (average 8.33), $(La/Yb)_N$ from 7.79×10^{-6} to 13.25×10^{-6} (average 10.52×10^{-6}), slightly negative Ce anomaly with δ_{Ce} varying from 0.805 to 0.850 (average 0.827) and obviously negative Eu anomaly with δ_{Eu} varying from 0.598 to 0.805 (average 0.702). The degree of LREE fractionation with $(La/Sm)_N$ from 3.41×10^{-6} to 4.93×10^{-6} (average 4.17×10^{-6}) is slightly higher than that of HREE with $(Gd/Yb)_N$ from 1.71×10^{-6} to 1.80×10^{-6} (average 1.75×10^{-6}).

To summarize, most orebodies in NM deposit have similar REE distributions and pattern with relative enrichment of LREE and distinct fractionation of LREE comparing with that of HREE, slightly negative Ce anomaly. However, the slight differences between them show that I orebody in inner contact nearby granite has distinct positive Eu anomaly and III orebody out of contact and occurred in the cranny among the carbonate stratum has higher REE concentrations than those of other orebodies.

4 Discussion

4.1 Magnetic intrusion

The metallogenic geological characteristics of NM deposit show that the metasomatic zoning for different skarn rocks is not distinct and the separation between skarn minerals and sulfides is insufficient, such as sphalerite, chalcocopyrite and other sulfides disseminated in hedenbergite rock from II-1 orebody or chalcocopyrite and magnetite distributed in garnet

rock from II-2 orebody, which is very different from the Gejiu skarn-typed tin deposit with clearly metasomatic zoning and massive orebody of sulfides^[9].

In contrast to the mineral association of different orebodies in NM deposit, I copper-zinc orebody in inner contact nearby granite with a lot of quartz and II-1 zinc-copper orebody in outer contact nearby limestone has quartz, calcite, fluorite and minor other minerals, which indicates that the volatile components should exist in post-magmatic hydrothermal fluid during its evolution. Previous studies have considered that only the high emplacement of granitic magmas with volatile components can form skarn and porphyry deposits, the presence of volatile components can make the fluid volume enlarged and always form explosion breccia and a series of cranny system on the top of granite body and in the wall rocks^[10]. The ore-bodies in NM deposit were mainly related to the high emplacement of Indosinian granite breaking through the carboniferous limestone, which caused the metallogenic system from closed state getting into half open state and destroyed the further transference and enrichment for metallogenic elements of post-magmatic hydrothermal fluid in their evolution, then all the metal sulfides deposited in contact or the tectonic cranny nearby country rock with strong metasomatism and alteration.

4.2 Fluid evolution

The metal elements including Cu, Fe, Zn and Pb of NM deposit have the distinct zoning in spacial distribution, i.e. Cu, Zn with chlorite and quartz from I orebody in inner contact nearby granite; Cu, Fe with andradite from II-1 orebody occurred in the western part of contact between granite

and limestone; Zn, Cu with hedenbergite and minor fluorite from II-2 orebody in the eastern part of contact between granite and limestone; Cu, Zn with idocrase from III orebody developed in the cranny of south limestone. This phenomenon can be observed in many other skarn deposits^[11]. REE share the closely similar geochemical behaviors during geological processes, which can be used in distinguishing metallogenic materials from different sources by their geochemical tracing^[12-26]. Most orebodies in NM deposit have the similar REE distributions and slowly right declined pattern, which indicate that they were from the same origin related to the post-magmatic hydrothermal fluid after granite emplacement. In addition, due to their different spacial locations, the I orebody and III orebody show slight differences compared with II-1 and II-2 orebody, which indicates that the post-magmatic hydrothermal might be constantly added in and mixed with basin fluid when it rises up and enters into the cranny of country rocks during its evolution^[27].

The average data of REE concentrations, δ_{Ce} (0.831) and δ_{Eu} (2.21) in I copper-zinc orebody are clearly higher than the corresponding parameters of REE in II-1 and II-2 orebody. Most studies show that the positive Eu anomaly were closely related to hydrothermal activity^[22-26] and the hydrothermal fluid with high temperature and reducing property can be in favor of the enrichment of Eu^{2+} ^[26]. Therefore, we can conclude that the ore-forming fluid for I copper-zinc orebody with high concentrations of sulfides should be formed in the reducing environment with high temperature in the early stage of metallogenic fluid evolution.

II-1 and II-2 orebody have the similar feature with lower REE concentrations and obviously negative Eu anomaly due to their similar metallogenic environment. Generally, the crystal temperatures of hedenbergite is higher than that of andradite based on their crystal sequence, so the ore-forming temperature of II-1 orebody with volatile components may also be higher than that of II-2 orebody without volatile components. In addition, there were a lot of magnetite, hematite or limonite in II-2 orebody and II-1 orebody, which indicate that they were formed in a high oxidative environment.

Compared with other orebodies, the III copper-zinc orebody has the highest average data of REE concentrations (115.48×10^{-6}) and distinct fractionation of LREE and HREE as well as slight negative anomaly of δ_{Ce} (0.827) and δ_{Eu} (0.702), which exhibits that there were more basin fluid mixed with magmatic hydrothermal fluid in the later stage of metallogenic fluid evolution. With the temperature and pressure of metallogenic fluid declined, their metasomatic intensity with country rock of carbonate also weakened and the skarn minerals in III orebody mainly comprised the lower-grade metasomatic minerals such as idocrase and wollastonite.

5 Conclusions

(1) The metasomatic zoning for different skarn rocks, such

as andradite and hedenbergite, was not distinct in horizontal direction in NM deposit and most of sulfides were disseminated in andradite rocks or garnet rocks, which were mainly related to the high emplacement of Indosinian granite breaking through the top cover of Carboniferous limestone and caused the metallogenic system from closed state to half open state.

(2) All the orebodies in NM deposit were derived from a similar origin and mainly related to the coupling interaction between the post-magmatic hydrothermal fluid and basin fluid. The evolution of ore-forming fluid had the trend from reducing state in early stage to oxidative stage in later stage.

Acknowledgements: We wish to thank president Wang Jingbin, general manager Wang Side and other engineers from Beijing Donia Resources Co., Ltd. for help during fieldwork.

References:

- [1] Mo Xuanxue, Deng Jinfu, Dong Fangliu, Yu Xuehui, Wang Yong, Zhou Su, Yang Weiguang. Volcanic petrotectonic assemblages in sanjiang orogenic belt, S W China and implication for tectonics. *Geological Journal of China Universities* (in Chin.), 2001, 7(2): 121.
- [2] Pow-foong Fan. Accreted terranes and mineral deposits of Indochina. *Journal of Asian Earth Sciences*, 2000, (18): 343.
- [3] Tang Shirong. The general situation of mineral resource in Laos. *Yunnan Geology* (in Chin.), 1994, 13(4): 392.
- [4] Schwartz M O, Rajah S S, Askury A K, Putthapiban P, Djaswadi S. The southeast Asian tin belt. *Earth-Science Review*, 1995, 38: 95.
- [5] Jia Runxing, Fang Weixua, He Ying, Gao Zhenmin, Li Hongyang. Geochemical characteristics of rare earth elements in Gejiu tin polymetallic deposits, Yunnan Province, China. *Journal of Rare Earths*, 2004, 22(5): 714.
- [6] Sun S S, McDonough W F. Chemical and isotopic systematics of oceanic basalts: implications for mantle composition and processes. In: Saunders A D, Norry M J. magmatism in the ocean Basins. London: Geological Society Special Publication, 1989. 313.
- [7] Zhuang Yongqiu, Wang Renzhong, Yang Shupe, Yi Jiming. *Geology of Gjiu Tin-Copper Polymetallic Deposit*. Beijing: Seismological Press (in Chin.), 1996. 1.
- [8] Wang Zhonggang, Yu Xueyuan, Zhao Zhenhua. *Geochemistry of Trace Earth Element*. Beijing: Science Press (in Chin.), 1989. 349.
- [9] Jia Runxing, Fang Weixuan, Hu Ruizhong, Ma Zhenfei. Geological and geochemical characteristics of skarns from the tin polymetallic deposit, Gejiu district, Yunnan province, China. *Geological Review* (in Chin.), 2007, 53(2): 281.
- [10] Rui Zongyao, Zhao Yiming, Wang Longsheng, Wang Yitian. Role of volatile components in formation of skarn and porphyry deposit. *Mineral Deposits* (in Chin.), 2003, 22(1): 141.
- [11] Zhao Yiming. Metasomatic zoning in some major Pb-Zn polymetallic skarn deposits of China. *Mineral Deposits* (in Chin.), 1997, 16(2): 120.
- [12] Yang Xueming, Yang Xiaoyong, Chen Tianhu, Zhang Peishan, Tao Kejie, Le Bas J, Henderson P. Geochemical characteristics of a carbonatite dyke rich in rare earths from Bayan Obo,

- China. *Journal of the Chinese Rare Earth Society* (in Chin.), 1999, **17**(4): 289.
- [13] Pang Jiangli, Sun Gennian. Geochemical behaviour of rare earth elements in Jianchaling deposit, Shaanxi province. *Journal of the Chinese Rare Earths Society* (in Chin.), 1999, **17**(4): 359.
- [14] Pang Jiangli. Geochemistry of rare earth elements in hydrothermal ore deposit in Heishan area, Shaanxi province. *Journal of Rare Earths*, 1999, **19**(1): 53.
- [15] Huang Zhilong, Xiao Huayun, Xu Cheng, Liu Congqiang. Geochemistry of rare earth elements in lamprophyres in Laowangzhai gold orefield, Yunnan province. *Journal of Rare Earths*, 2000, **18**(1): 62.
- [16] Chen Tianhu, Yang Xueming, Yue Shucang, Li Shuangying, Wang Daoxuan. Geochemistry of rare elements in Xikeng Ag Pb Zn ore deposit, South Anhui, China. *Journal of Rare Earths*, 2000, **18**(3): 169.
- [17] Yuan Feng, Zhou Taofa, Liu Xiaodong, Yue Shucang. Geochemistry of rare earth elements of Anqing copper deposit in Anhui province. *Journal of Rare Earths*, 2002, **20**(3): 223.
- [18] Wang Min, Sun Xiaoming, Ma Mingyang. Rare earth elements compositions and genesis of Xinhua large scale phosphorite deposit in western Guizhou, China. *Journal of Rare Earths*, 2005, **23**(3): 323.
- [19] Xu Xiaochun, Lu Sanming, Xie Qiaoqin, Chu Guozheng, Xiong Yaping. Rare earth element geochemistry on magmatic rocks and gold deposits in Shizishan ore-field of Tongling, China. *Journal of Rare Earths*, 2006, **24**(5): 617.
- [20] Xie Qiaoqin, Xu Xiaochun, Li Xiaoxuan, Chen Tianhu, Lu Sanming. Rare earth elements geochemistry of Laowan gold deposit in Henan province: Trace to source of ore-forming materials. *Journal of Rare Earths*, 2006, **24**(1): 115.
- [21] Philip R W, James F O. Rare earth element metasomatism in hydrothermal systems: The Willsboro-Lewis wollastonite ores, New York, USA. *Geochimica et Cosmochimica Acta*, 1998, **62**(17): 2965.
- [22] Fang Weixuan, Yang Shefeng, Liu Zhentao, Wei Xinglin, Zhang Baochen. Geochemical Characteristics and significance of major elements, trace elements and REE in mineralized altered rocks of large-scale Tsagaan Suvarga Cu-Mo Porphyry deposit in Mongolia. *Journal of Rare Earths*, 2007, **25**(6): 759.
- [23] Zhao Bin, Zhao Jinsong, Liu Haichen. REE geochemical studies of whole rock and rock forming minerals in skarns from Cu (Au), Cu-Fe(Au) and Fe ore deposits distributed along middle-lower reaches of Yangtze River, China. *Geochemica* (in Chin.), 1999, **28**(2): 113.
- [24] Tian Shihong, Ding Tiping, Hou Zengqian, Yang Zhusen, Xie Yuling, Wang Yanbin, Wang Xuncheng. REE and stable isotope geochemistry of the Xiaotongguanshan copper deposit, Tongling, Anhui. *Geology in China* (in Chin.), 2005, **32**(4): 604.
- [25] Zhao Jinsong, Qiu Xuelin, Zhao Bin, Tu Xianglin, Yu Jue, Lu Tieshan. REE geochemistry of mineralized skarns from Daye to Wushan region, China. *Geochemica* (in Chin.), 2007, **36**(4): 400.
- [26] Yin Haisheng, Lin Jinhui, Zhao Xixi, Zhou Kenken, Li Junpeng, Huang Huagu. Geochemistry of rare earth elements and origin of positive europium anomaly in Miocene-Oligocene Lacustrine Carbonates from Tuotuohe basin of Tibetan plateau. *Acta Sedimentologica Sinica* (in Chin.), 2008, **26**(1): 1.
- [27] Yang Guangshu, Wen Hanjie, Hu Ruizhong, Qin Chaojian, Yu Wenxiu. Fluid inclusions of Anqing skarn-type Fe-Cu deposit, Anhui Province. *Geochemica* (in Chin.), 2008, **37**(1): 27.